Proceedings of IMECE2006
2006 ASME International Mechanical Engineering Congress and Exposition
November 5-10, 2006, Chicago, Illinois, USA

IMECE2006-14711

AN INVESTIGATION OF A MICRO-SCALE RANQUE-HILSCH VORTEX TUBE

Amar F. Hamoudi
Department of Mechanical, Automotive and Materials Engineering
University of Windsor, Windsor, Ontario, Canada
elubaidi@gmail.com

Amir Fartaj
Department of Mechanical, Automotive and Materials Engineering, University of Windsor,
Windsor, Ontario, Canada
fartaj@uwindsor.ca

Gary W. Rankin
Department of Mechanical, Automotive and Materials Engineering, University of Windsor,
Windsor, Ontario, Canada
rankin@uwindsor.ca

ABSTRACT

The results of an experimental investigation of the energy separation performance of a micro-scale Ranque-Hilsch vortex tube are presented in this paper. The micro-scale vortex tube is 2 mm in diameter and constructed using a layered technique from multiple pieces of Plexiglas and aluminum. Four inlet slots, symmetrically located around the tube, form the vortex. The hydraulic diameter of each inlet slot and the orifice diameter for the cold exit are 229 and 800 microns respectively. The working fluid is low pressure, non-dehumidified compressed air at room temperature. The rate of the hot gas flow is varied by means of a control valve to achieve different values of cold mass fraction. The mass flow rates, temperatures and pressures of the supply and outlet flows are measured and the performance of the device presented. The supply channel Reynolds number is varied over a considerable range which extends into the laminar regime in order to determine the operating conditions for cooling. An increase in dimensionless temperature is found in both the cold and hot outlets as supply nozzle Reynolds number increases from zero. Maximum values occur at a Reynolds number of approximately 500 and the cold flow dimensionless temperature becomes negative at about 2500. Although the optimum cold mass ratio is higher than the conventional tubes, the effect on performance of tube length and cold exit diameter is similar to the conventional devices.

KEY WORDS

Ranque-Hilsch effect, temperature separation, micro-fluidics, vortex cooling.

INTRODUCTION

The development of new micro-fabrication techniques has led to a resurgence of research in micro-fluidic devices. The devices that have received most attention in the literature include pumps, valves, flow sensors and heat exchangers [1]. The performance of micro-scale Ranque-Hilsch tubes, non-moving part pneumatic devices that separate cold fluid from hot fluid for the purpose of cooling, has not received much attention. Traditionally, the vortex tube has been used in many low temperature applications where the efficiency is not the most important factor. For example, the vortex tube has been used to cool parts of machines, dehumidify gas samples, cool electronic control enclosures as well as chill environmental chamber and test temperature sensors. A micro-scale Ranque-Hilsch tube in combination with a micro-fluidic pump has potential application in the cooling of electronic chips.

The phenomenon of temperature separation occurring inside a cylindrical tube was reported for the first time by a French physicist, G. Ranque, who applied for a US patent in December 1932 [2] and subsequently presented a paper to the French Society of Physics in 1933 [3]. The discovery was further advanced, in 1947, by R.Hilsch [4] who published some constructional details of the vortex tube along with the performance curves of the device for different tube diameters at various operating conditions. The vortex tube is a very simple device without moving parts (i.e. diaphragm, pistons, shafts, etc.) as shown in Fig. 1. In this arrangement a stream of a compressed gas (usually air) is injected tangentially into the vortex tube having diameter *D* using one or more nozzles symmetrically located around the tube. The injected flow accelerates at the entrance establishing a strong swirl flow

which causes a region of increased pressure near the wall and a region of decreased pressure near the axis.

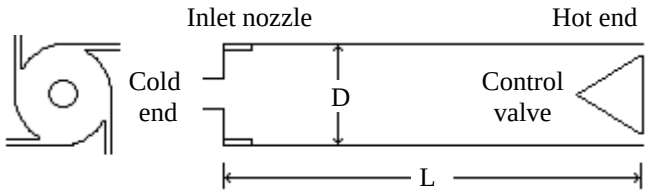

Fig. 1 Vortex tube schematic drawing

The presence of an end wall alongside the inlet nozzles forces some of the injected gas to flow axially in a helical motion toward the far end of the tube (the hot end) where a control valve is located. In the usual operation of this device, the flow through the hot end is restricted by partially closing the control valve. This causes even the low pressure at the center of the tube to be higher than atmospheric and hence flow exits the central orifice in the end wall. This also causes some of the flow that had been directed to the far end of the tube to reverse direction along the center of the tube and also leave the tube through the central orifice (Fig. 2). The gas escaping near the tube wall at the far end of the inlet nozzles has higher stagnation temperature than the incoming gas and the gas exiting through the central orifice has a lower stagnation temperature than the inlet gas.

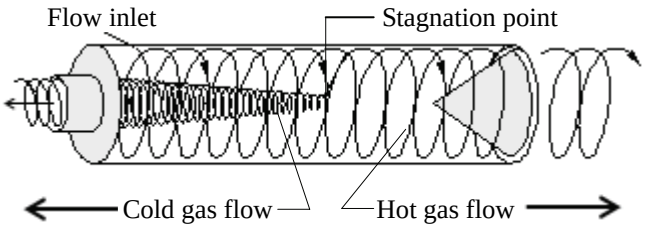

Fig. 2 Hot and cold rotating streams in a counter flow vortex tube

A very low temperature can be obtained from the cold end by operating the device at a supply pressure of a few atmospheres. For example, Hilsch [4] operated a 9.6 mm diameter tube using compressed air at approximately 600 kPa inlet pressure and 293 K inlet temperature to produce a cold temperature, T_c, of 245 K. The temperatures of the hot and the cold stream are varied by properly changing the cold mass ratio, $\dot{m}_c / \dot{m}_o$, which can be entirely regulated through the control valve located at the hot exit.

LITERATURE REVIEW

The most recent review of the literature related to the Ranque-Hilsch tube is given in the dissertation by Gao [5]. Previous reviews [6,7 and 8] reveal hundreds of papers dealing with this topic. Only those papers pertinent to this study will be mentioned in the following.

In spite of the large volume of research that has been devoted to this subject over the years, there is still disagreement regarding the mechanism that accounts for the operation of this device. Although it has been shown that energy separation can occur in laminar flow [9,10] most explanations involve turbulent fluctuations [11]. Kurosaka [12] gives an acoustic streaming explanation while others claim that the operation is based on secondary flows and a thermodynamic refrigeration cycle [13].

The only study that was specifically directed towards micro-scale vortex tube devices was that of Dyskin and Kramarenko [14]. They reported experimentally determined performance characteristics (adiabatic efficiency) for vortex tubes operating with a pressure ratio of 6 with diameters of 1, 2 and 3 mm. The corresponding mass flow rates were 14.3 x 10^{-5}, 40.0 x 10^{-5} and 94 x 10^{-5} kg/sec respectively. Although details of the geometry are not given, an estimate of the inlet Reynolds numbers used for these cases yield values greater than 6000. It was, however, noted that the cooling effect decreased with decreasing flow rate. This is consistent with the speculation of Negm et al. [15] that the cooling effect should decrease with decreasing Reynolds number.

RESEARCH OBJECTIVE

The objective of this work is to experimentally investigate the characteristics of a vortex tube at supply channel Reynolds numbers that extend from the laminar into the turbulent flow regime in order to determine the minimum operating conditions of these devices for cooling applications. In addition, the effect of tube length and cold outlet orifice size on the performance characteristic of micro-scale vortex tubes will be determined.

APPARATUS DESCRIPTION

The 2 mm diameter micro-scale vortex tube, constructed at the technical support center of the University of Windsor using a layered technique from multiple pieces of Plexiglas and aluminum is shown in Fig. 3. The working fluid is filtered low pressure, non-dehumidified, compressed air.

The hydraulic diameter of the inlet slots and the orifice diameter of the cold exit are 229 and 800 microns respectively. The hot gas flow rate is varied by means of a control valve to achieve different values of cold mass fraction y_c. The length of the tube and hence the *L/D* ratio was increased by adding a number of layers of Plexiglas. In addition, a number of cold end plates are available with different orifice diameters. As depicted in Fig. 4, the compressed air line is connected to the inlet nozzle (1) attached to the body of the nozzle section of the vortex tube. A longitudinal hole (2) is provided to connect the inlet nozzle to a 4 x 3 mm channel (3) that acts as a manifold with a pressure very close to that measured at the inlet nozzle (1). The vortex is formed by four inlet slots each of size 0.3822

mm x 0.1635 mm (4) that are symmetrically located around the tube (5).

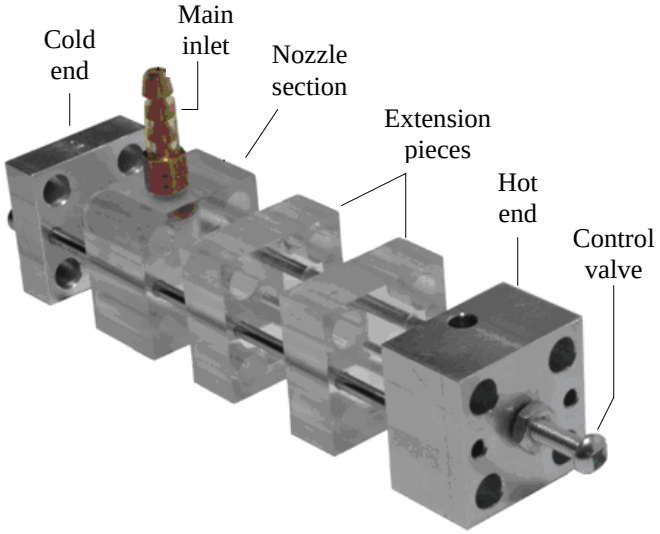

Fig. 3 Expanded view of the micro-scale vortex tube

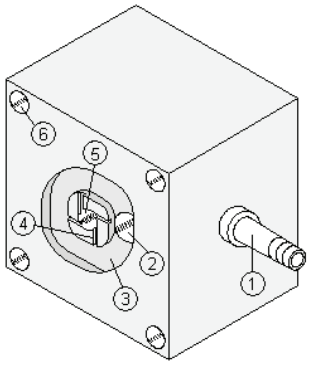

Fig. 4 Nozzle section of the vortex tube

The multiple layers forming the vortex tube were aligned using two stainless steel guide pins so that the rotating flow would not be disturbed while traversing along the length of the tube. The Plexiglas layers were sandwiched between two aluminum pieces which represent the hot and the cold end of the vortex tube. Four stainless steel bolts were located in longitudinal holes at the corners of each piece (6) and nuts were used to tighten the pieces of the vortex tube.

EXPERIMENT SETUP

The experimental test facility used for this study is shown schematically in Fig. 5. Low-pressure compressed air was passed through a control valve (1), 5-micron air filter (2) and a pressure-regulating valve (3) before entering the vortex tube. A water manometer (4) was used to accurately measure (with an uncertainty of ± 0.01 kPa) the low supply pressure which ranged from 2 to 17.5 kPa. A pressure gage with an uncertainty of ± 3 kPa was used for the pressures above this range. The temperatures of the inlet, cold and hot air are measured using type T thermocouples located at (5), (8) and (11) respectively. These thermocouples were calibrated using an ice bath and boiling water and the estimated uncertainty in measurement is ± 0.4 K.

Low pressure compressed air was injected into the vortex tube through the manifold (6) and then the inlet slot (7). The cold exit pressure, P_c, and hot exit pressure, P_h, were measured using digital manometers (9) and (12).

The volumetric flow rate of air exiting the cold and the hot openings were measured using separate rotameters (10) and (13). The rotameters were calibrated while connected to the apparatus so that both were subjected to the same working pressures as encountered in the experiment to avoid the need for corrections. The uncertainty in the measurements of both the hot and cold volume flow rates is ± 1.0 x 10^{-6} m^3/s.

Assuming an ideal gas, the density of the hot and the cold gas was calculated using the equation of state:

$$\rho = \frac{P}{RT} \tag{1}$$

Atmospheric pressure and temperature were measured to an uncertainty of ± 0.7 kPa and ± 0.5 K respectively. This gives an uncertainty in density of ± 2.3 x 10^{-3} kg/ m^3. The method of Kline and McKlintock [16] was used to determine the propagation of uncertainties.

The inlet Reynolds number was calculated as follows:

$$\mathrm{Re} = \frac{\dot{m}\, d_n}{4\, A\, \mu} \tag{2}$$

where d_n is the equivalent diameter of the inlet nozzle, A is the cross-sectional area of one inlet nozzle, and μ is the viscosity of the inlet air which is taken to be 1.82 x 10^{-5} kg/m s. This results in an uncertainty of Re in the range ± (75 – 230). The cold air mass ratio, y_c, is defined as:

$$y_c = \frac{Cold\ gas\ mass\ flow\ rate}{Total\ inlet\ gas\ mass\ flow\ rate} \tag{3}$$

and has an uncertainty in the range ± (0.01 – 0.12).

Due to the low operating pressures in the experiments conducted using this facility, adjustment of the cold air mass ratio using the control valve placed at the hot end significantly altered the exit pressures of the cold and hot exits due to the resistance of the rotameters. Each was altered by a different amount which effectively created a different exit pressure in each case. To avoid this problem, the flow of the cold or the

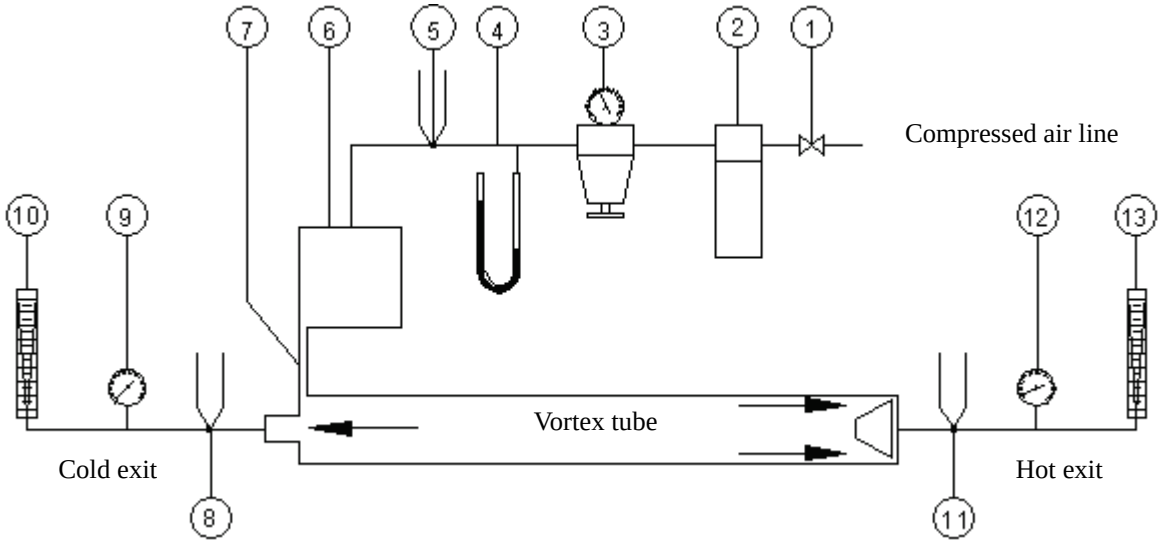

Fig. 5 Experimental test facility

hot air stream was restricted with a flow restriction device in such a manner that the pressure of the cold and hot air exit flows was almost equal.

The temperatures measured using the thermocouples were assumed to be equal to the total temperature. This can be justified since the total temperature is defined as:

$$T_t = T_s + \frac{u^2}{2c_p} \tag{4}$$

where c_p is the specific heat of the inlet air at constant pressure and is taken as 1005 J/kg K, the subscripts *t* and *s* represent the total and the static temperatures respectively and the term $u^2/2c_p$ is very small. Within the range of the working pressure used in this experiment (i.e.: 2.5 – 103 kPa) and 293.1 K inlet temperature, the cold and the hot exit velocities were found to be in the range of 0.15–1.84 m/s and 0.14-1.08 m/s respectively and the maximum dynamic temperatures calculated for both cold and hot temperature were 1.7×10^{-3} and 5.8×10^{-4} K respectively.

In the first series of tests, the performance characteristics of the vortex device were determined at fix geometry. This meant that the control valve opening was kept constant throughout the tests as the supply pressure was varied. The measured cold and hot temperature plotted in a dimensionless manner for various Reynolds numbers is shown in Fig. 6. The uncertainties in this figure and the remaining figures are indicated by the error bars unless they are within the size of the symbol.

The minimum total flow rate was 9.86×10^{-6} kg/s which results in a Reynolds number of 500. It can be seen that, at this low Reynolds number, both hot and cold exit temperatures are higher than the inlet temperature, T_o. The trend of the curves at Reynolds number below 500 was estimated as shown in the dashed line as it is known that all temperatures must be equal for the case of no flow. At this low Reynolds number, the vortex motion is not likely well established and the effect of the viscous term is the dominating factor. The viscous dissipation, therefore, causes the rise in the temperatures of both outlet streams.

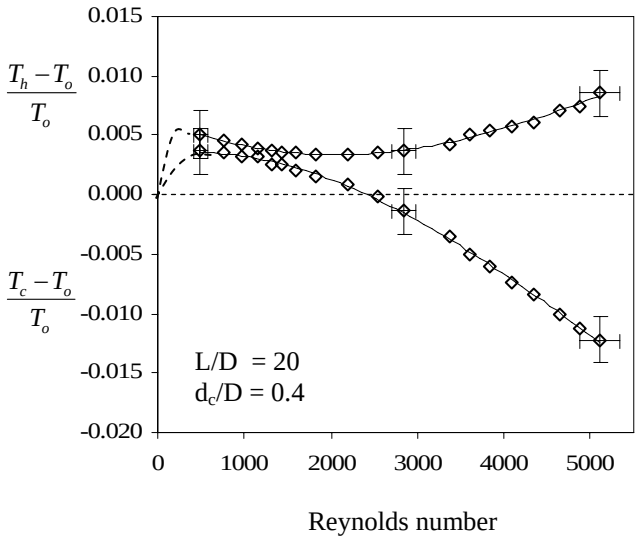

Fig. 6 Temperature separation at low Reynolds number.

It is interesting to observe that the cooling effect begins to appear at a value of the inlet Reynolds number of approximately 2500 (Fig. 6) which corresponds, roughly, to the transition from laminar to turbulent flow in fully developed pipe flow. The trend of increasing temperatures with Reynolds number, however, is reversed at a much lower Reynolds number of approximately 500. This is consistent

with the reduction in the critical Reynolds number estimated for tube lengths shorter than that required for fully developed flow which is common to micro-fluidic devices [1].

A plot of the inlet pressure versus Reynolds number is shown in Fig. 7. The trend is as expected.

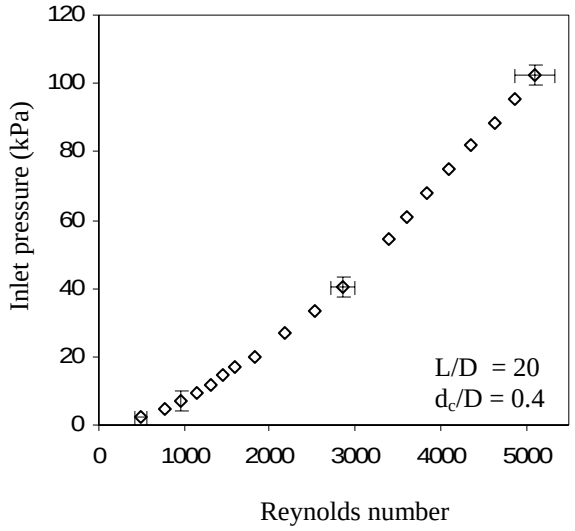

Fig. 7 Inlet pressure as a function of Reynolds number

The variation of the cold air mass ratio is shown in Fig. 8. It is noted to increase with Reynolds number up to a value of Reynolds number equal to 1000, above which it remains almost constant.

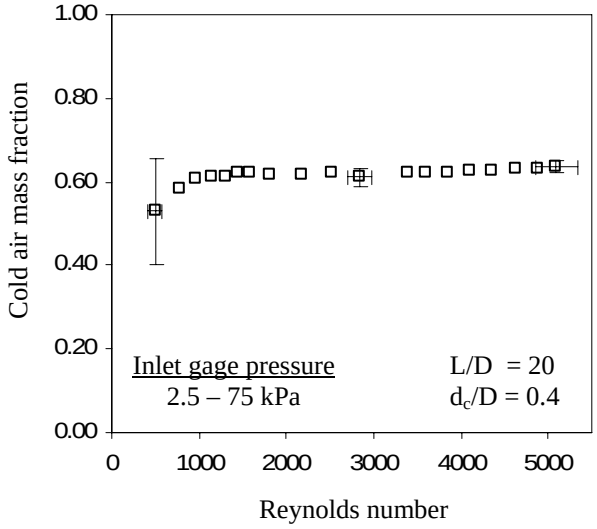

Fig. 8 Cold air mass ratio versus Reynolds number

The next set of experiments involved observing the cold and hot output flow temperature variation at an inlet air temperature of 293.1 K while changing the cold air mass ratio and holding the inlet Reynolds number constant at values of approximately 1000, 2500 and 4000. The results are shown in Fig. 9 in a dimensionless form that takes into consideration the effect of changes in the inlet temperature. At a Reynolds number of 1000, both hot and cold temperatures are above the inlet temperature and the variation of each as a function of the cold air mass ratio is insignificant. The variations of the cold and the hot temperature are more significant at Reynolds numbers of 2500 and 4000. This is consistent with the performance of the micro-scale vortex tubes investigated by Dyskin and Kramarenko [14] and speculated by Negm et al. [15].

EFFECT OF OPERATING CONDITIONS

The micro-scale vortex tube investigated at low Reynolds number is operated at higher working pressures in order to make a comparison with the results of Dyskin and Kramarenko [15]. The cold and the hot temperature differences ($T - T_o$) obtained at 400 kPa inlet pressure and 294 K inlet temperature, which correspond to an inlet Reynolds number slightly over 15,000, are found to be –19.1 K and 17 K respectively. This is consistent with the observations of Dyskin and Kramarenko [14] and indicates the same conclusion regarding the ability of the micro-scale vortex tube to operate as a cooling device.

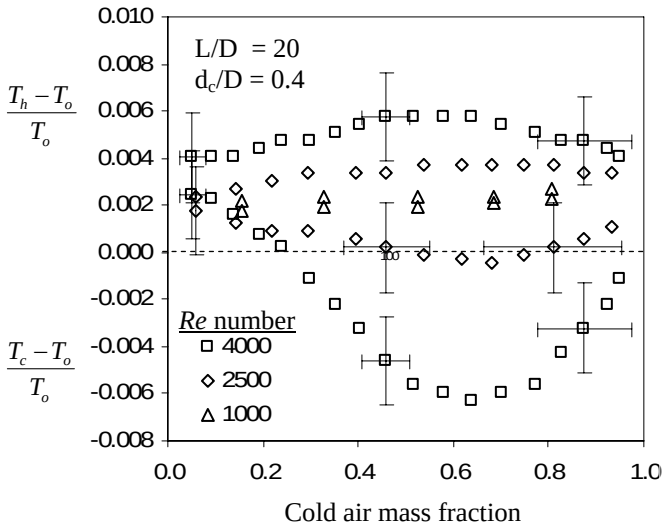

Fig. 9 Dimensionless cold and hot temperature as a function of the cold air mass ratio.

The performance of the micro-scale vortex tube is also investigated at a number of higher inlet pressures for different values of the cold air mass ratio. The inlet pressures considered are 100, 200, 300 and 400 kPa at an average inlet temperature of 293.6 K and the cold air mass ratio is systematically varied from 0.05 to 0.95. The dimensionless hot and cold temperature as a function of the cold air mass ratio and as a function of the inlet pressure is shown in Fig.

10. An increase in the inlet pressure is seen to cause the values of the dimensionless cold temperature difference to increase over the whole range of the cold air mass fraction. The value of the cold air mass ratio corresponding to the minimum cold air stream temperature decreases with increasing supply pressure from 0.6 at 100 kPa to 0.5 at 400 kPa. It is not expected for this value to reach range of 0.3 to 0.45 as observed in conventional vortex tubes [15]. Recent experimental data, not included in this paper, seems to indicate that this difference is more related to the relative size of the inlet nozzle hydraulic diameter to the cold orifice diameter than to the micro-scale of the device. Similarly, the maximum hot air temperatures seem to be at values of cold mass ratio different than those for the conventional devices.

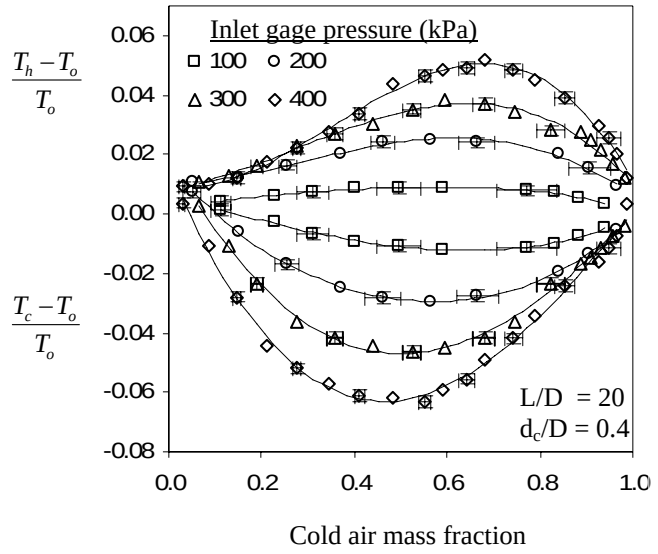

Fig. 10 Dimensionless hot and cold temperature as a function of cold air mass fraction and inlet pressure

EFFECT OF GEOMETRY

In this section only the temperature drop is considered as these devices have their primary application in cooling.

Figure 11 gives the relationship between temperature drop of the cold flow and the dimensionless tube length. It can clearly be seen that by increasing the tube length and hence the *L/D* ratio, the cold temperature drops. The trend of the curve indicates that longer tube lengths could possibly result in better performance. Dyskin and Kramarenko [14] found an optimum L/D of 60 which is consistent with that found for conventional vortex tubes [17]. Given the range of the current data, this optimum cannot be confirmed or disputed.

Figure 12 gives the relationship between temperature drop of the cold flow and the dimensionless orifice diameter. It is seen that increasing the d_c/D ratio results in a decrease in the dimensionless temperature drop of the cold air streams. This indicates that the best d_c/D ratio is larger than 0.4. This is consistent with the conventional devices [17].

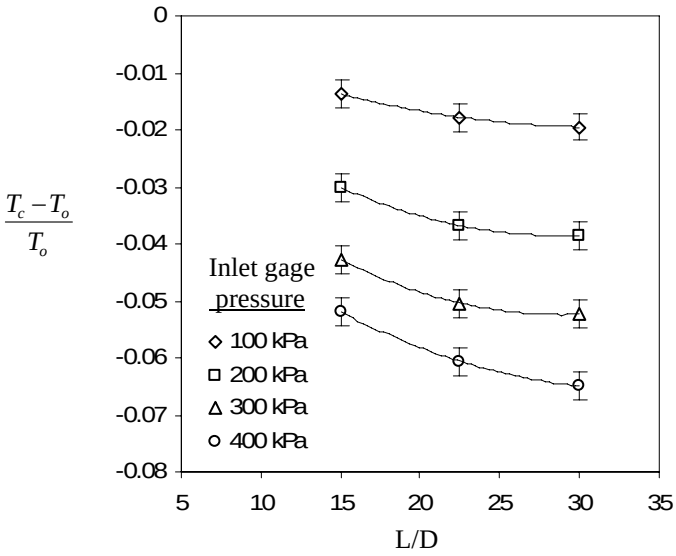

Fig. 11 Maximum dimensionless cold temperature drop versus *L/D* ratio.

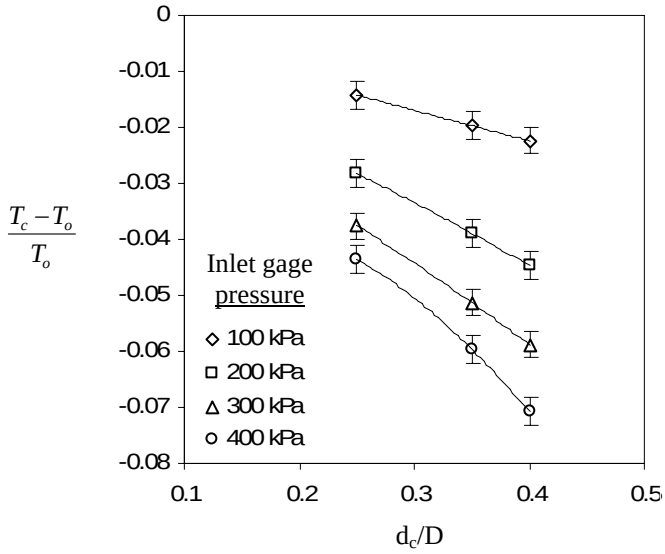

Fig. 12 Maximum dimensionless cold temperature drop versus d_c/D ratio.

CONCLUSIONS

Experiments conducted on a micro-scale vortex tube at low Reynolds numbers, based on the inlet tube hydraulic diameter and average velocity, exhibit an increase in dimensionless temperature in both the cold and hot outlets as the Reynolds number increased from zero reaching maximum values before a Reynolds number of 500. In the case of the hot outlet, the dimensionless temperature decreases after reaching its maximum and achieves a minimum value at a Reynolds number of approximately 2000. It then increases steadily with further increases in Reynolds number. The cold outlet

dimensionless temperature decreases steadily after the maximum to become negative at a Reynolds number of approximately 2500. This implies that there is no cooling effect at Reynolds numbers consistent with laminar flow.

Except for very low Reynolds numbers the cold mass fraction is approximately constant as the Reynolds number increases for a fixed geometry and control valve setting. As the control valve setting is changed, the optimum cold mass fraction is found to be in the range of 0.45 to 0.6. The effect of dimensionless tube length and cold exit orifice diameter on micro-scale vortex tube performance is similar to that in the conventional devices.

NOMENCLATURE

A	cross section area of the inlet slot
c_p	specific heat at constant pressure
D	vortex tube inner diameter
d_c	cold exit (orifice) diameter
d_n	equivalent diameter of the inlet slot
L	vortex tube length
$\dot{m}$	mass flow rate
P	pressure
R	gas constant
T	temperature
u	axial velocity
y_c	cold gas mass flow ratio

Greek Symbols

ρ	density
μ	dynamic viscosity
η	efficiency
v	kinematics viscosity

Subscripts

s	static
t	total
c	cold
h	hot
o	inlet

ACKNOWLEDGMENTS

The project was mainly funded and supported through Discovery Grants from the Natural Sciences and Engineering Research Council of Canada (Grant Numbers: OGP0001403 and OGP0105727).

REFERENCES

[1] Gravesen, P., Branebjerg, J., and Jensen, O.S., 1993, "Microfluidics—a review," J. Micromech. Microeng, **3**, pp. 168-182.

[2] Ranque, G., Method and apparatus for obtaining from a fluid under pressure two currents of fluids at different temperatures. Application date December 6, 1932. U.S. patent number 1,952,281.

[3] Ranque, G., 1933, "Expériences sur la détente giratoire avec productions simultanées d'un énchappement d'air chaud et d'un énchappement d'air froid", Journal de Physique et de la Radium, **4,** pp. 1125–1155.

[4] Hilsch, R., 1947, "The use of the expansion of gases in a centrifugal field as cooling process", Review of Scientific Instruments, **18 (2)**, pp. 108–113.

[5] Gao, C., 2005, Experimental study on the Ranque-Hilsch vortex tube, Ph.D. Dissertation, Department of Applied Physics, Eindhoven University of Technology, The Netherlands.

[6] Cockerill, T.T., 1998, Thermodynamics and fluid mechanics of a Ranque-Hilsch vortex tube, Masters Thesis, Department of Engineering, University of Cambridge, England.

[7] Westley, R., 1954, A bibliography and survey of the vortex tube, Cranfield College Note 9, College of Aeronautics.

[8] Soni, Y., 1973, A parameteric study of the Ranque-Hilsch tube. Ph.D. dissertation, University of Idaho Graduate School, U.S.A.

[9] Kassner, R. and Knoernschild, E., 1948, "Friction laws and energy transfer in circular flow", Wright-Patterson Air Force Base, Technical report No. F-TR-2198-ND.

[10] Deissler, R.G and Perlmutter, M., 1958, "An analysis of the energy separation in laminar and turbulent compressible vortex flows". Heat Transfer and Fluid Mechanics Institute, Stanford University Press, pp. 40-53.

[11] Deissler, R.G and Perlmutter, M., 1960, "Analysis of the flow and energy separation in a turbulent vortex", International Journal of Mass and Heat Transfer, **1**, pp. 173-191.

[12] Kurosaka, M., 1982, "Acoustic streaming in swirling flow and the Ranque-Hilsch (vortex-tube) effect", Journal of Fluid Mechanics, **124**, 139–172.

[13] Ahlborn, B., Keller, J.U. and Rebhan, E., 1998, "The heat pump in a vortex tube", Journal of Non-Equilibrium Thermodynamics, **23(2)**, 159–165.

[14] Dyskin, M., Kramarenko, P., 1984, “Energy characteristics of vortex microtube”, Journal of Engineering Physics and Thermophysics, **47 (6)**, pp. 1394-1395

[15] Negm, N., Seraj, A., Abull Ghani, S., 1988, “Generalized correlations for the process of energy separation in vortex tube”, Modeling, simulation and control, B, AMSE Press, **14 (4)**, pp. 47-64.

[16] Kline, S. J., and McClintock, F. A., 1953, “Describing uncertainties in single-sample experiments”, Mechanical Engineering, **75**, pp. 3-8.

[17] M.H. Saidi; M.S. Valipour, 2003, “Experimental modeling of vortex tube refrigerator”, Applied Thermal Engineering, **23**, pp. 1971-1980.